Extreme lunar surface charging during solar energetic particle events

J. S. Halekas,[1] G. T. Delory,[1] D. A. Brain,[1] R. P. Lin,[1,2] M. O. Fillingim,[1] C. O. Lee,[1]
R. A. Mewaldt,[3] T. J. Stubbs,[4,5] W. M. Farrell,[5] and M. K. Hudson[6]

[1] We analyzed a series of solar energetic particle events in late April and early May of 1998, during which lunar surface potentials reached values as large as ~-4.5 kV (the largest recorded by Lunar Prospector). The two largest surface charging events during this time period correspond to energetic particle injections, when the electron flux between 50 keV and 5 MeV exceeded the proton flux over the same energy range. We searched the entire Lunar Prospector data set for other large negative surface charging events, and found that they occur almost exclusively during magnetotail crossings (when the Moon encounters the plasmasheet) and solar energetic particle events. Lunar surface charging (and its effect on the lunar dust environment) during inherently unpredictable space weather events represents a significant hazard for exploration. **Citation:** Halekas, J. S., G. T. Delory, D. A. Brain, R. P. Lin, M. O. Fillingim, C. O. Lee, R. A. Mewaldt, T. J. Stubbs, W. M. Farrell, and M. K. Hudson (2007), Extreme lunar surface charging during solar energetic particle events, *Geophys. Res. Lett.*, *34*, L02111, doi:10.1029/2006GL028517.

1. Introduction

[2] Although we often think of the lunar environment as essentially static, it is in fact very electrically active. The Moon has a minimal atmosphere and only localized weak crustal magnetic fields, leaving its surface essentially directly exposed to the impact of solar UV and X-rays as well as solar wind plasma and energetic particles. This creates a complex lunar electrodynamic environment, with the surface typically charging positive in sunlight and negative in shadow, to potentials that vary over orders of magnitude in response to changing solar illumination and plasma conditions.

[3] One expects the largest surface potentials to occur on the lunar night side, where photoemission is absent, and ambient plasma currents primarily drive surface charging [*Manka*, 1973]. Before the Lunar Prospector (LP) mission, few measurements of nightside potentials existed, but LP measurements have now allowed us to place some constraints upon their magnitude. LP data indicate charging of the lunar surface to potentials on the order of ~-100 V or less in the solar wind wake and magnetospheric tail lobes [*Halekas et al.*, 2002]. Meanwhile, in the magnetospheric plasmasheet, a region of high-temperature plasma, LP measurements indicate lunar surface potentials occasionally as high as -2 kV [*Halekas et al.*, 2005a].

[4] Solar energetic particle (SEP) events at the Moon have been considered previously from a hazard standpoint because of the associated high-energy radiation, with up to half of all energetic particles that strike the Moon during a solar cycle arriving during a few large events [*Adams and Shapiro*, 1985]. These events produce some of the most disturbed and energetic plasma conditions found around the Moon; however their effects on lunar surface charging have not yet been considered in detail. We now use LP data to investigate lunar surface charging during SEP events.

2. Lunar Surface Charging Observations

[5] When the lunar surface charges negative, it has two effects on the electron distribution measured by an orbiting spacecraft such as LP, when it is magnetically connected to the surface [see *Halekas et al.*, 2002]. First, parallel electric fields alter the boundary in phase space (the so-called loss cone) between electrons that reach the surface (and are absorbed) and those that reflect adiabatically. In the absence of parallel electric fields, the loss cone boundary does not depend on electron energy, but when a potential difference exists between the surface and LP this loss cone has a characteristic variation with energy. Second, plasma electrons that impact the surface produce low-energy secondary electrons efficiently, with yields close to or even exceeding unity for some incident electron energies [*Horanyi et al.*, 1998]. Secondary electrons are accelerated upwards by parallel electric fields, forming a high-flux field-aligned beam of electrons with energies corresponding to the potential difference between the surface and LP.

[6] Either of these diagnostic features of the electron distribution can be used to infer negative lunar surface potentials, and the two methods have been shown to agree well [*Halekas et al.*, 2002]. During SEP events, high energy particles penetrate the LP Electron Reflectometer (ER) housing, greatly increasing the background count rate. These penetrating particles make a precise measurement of the energy dependence of the loss cone difficult. Therefore, in this study, we primarily utilized accelerated secondary electron beams as a diagnostic of negative lunar surface charging.

[7] As an illustrative example, Figure 1 shows an electron distribution measured during an SEP event in May, 1998. The distribution is extremely noisy, due to penetrating particle counts, but one can still identify a loss cone around 180° pitch angles, for upward-going electrons with energies

---

[1]Space Sciences Laboratory, University of California, Berkeley, California, USA.
[2]Physics Department, University of California, Berkeley, California, USA.
[3]California Institute of Technology, Pasadena, California, USA.
[4]Goddard Earth Sciences and Technology Center, University of Maryland Baltimore County, Baltimore, Maryland, USA.
[5]NASA Goddard Space Flight Center, Greenbelt, Maryland, USA.
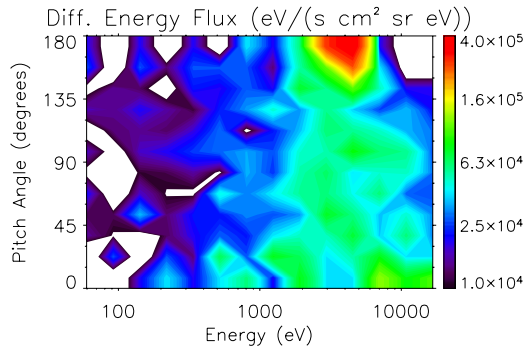[6]Department of Physics and Astronomy, Dartmouth College, Hanover, New Hampshire, USA.

Figure 1. Energy pitch angle spectrogram measured during an extreme charging event on May 6, 1998 at 10:45:41 UT, showing a high-flux field-aligned beam of upward-traveling electrons at ~4.5 keV, and a loss cone around 180° pitch angle at energies above 4.5 keV.

above ~7 keV. At energies just below this, we find a very high-flux field-aligned beam of electrons, with a center energy of ~4.5 keV. We can easily resolve this beam, even with the significant penetrating particle background. Since we expect that the LP spacecraft also charges negative in shadow, the potential difference of ~4.5 kV represents a lower limit on the magnitude of the negative lunar surface potential.

3. Charging During a Series of SEP Events

[8] We developed automated software to search for similar upward-traveling field-aligned electron beams throughout the LP mission (January 1998 – July 1999). This allowed us to identify all extreme charging events throughout this time period. The largest lunar charging event thus identified occurred during a series of SEP events in late April and early May of 1998, at a time when the Moon was in the solar wind and LP at ~100 km altitude. We show a selection of LP data and upstream data from ACE and SOHO during this series of events in Figure 2.

[9] Figures 2a and 2b show magnetic field magnitude and electron differential energy flux measured by LP. At energies below a few keV, counts are primarily due to electrons that follow the ER optics; however, above these energies counts from penetrating particles comprise a significant fraction of the recorded counts. Given the thickness of the ER housing, these penetrating particles could be either >~2 MeV electrons or >~10 MeV protons, with no a priori way to distinguish between these two possibilities.

[10] Figure 2c shows the peak secondary electron beam energy recorded on each LP orbit. During each two hour orbit, LP passes through the lunar plasma wake [*Halekas et al.*, 2005b]. We observe negative surface charging during every wake passage, when the lunar surface is shadowed and photoemission therefore absent. As discussed previously, the peak beam energy therefore represents a lower limit on the peak negative surface potential during each orbit. The peak beam energy for each orbit generally does not represent an isolated occurrence, but rather is representative of tens of measurements in the central wake on that orbit. We show only the peak beam energy for each orbit in order to reduce the data density on the plot.

[11] Figures 2d and 2e show upstream electron and ion data for selected energies, as measured by the SOHO COSTEP (500 keV and 1.8 MeV electrons, 540 keV and 4 MeV protons), ACE EPAM (45 keV and 139 keV electrons, 56 keV and 140 keV protons), and ACE SIS (>30 MeV protons, note different units from other measurements) experiments [*Muller-Mellin et al.*, 1995; *Gold et al.*, 1998; *Stone et al.*, 1998]. Figure 2f shows total upstream electron and ion fluxes, and the difference thereof, integrated over the energy range from 50 keV to 5 MeV.

[12] This time period is a very active one, with as many as three full halo CMEs and three partial CMEs [*Burlaga et al.*, 2001]. Wind and ACE observe three interplanetary shocks (S1, S2, S3), as well as several directional discontinuities (D1, D2, D3) [*Farrugia et al.*, 2002]. A large magnetic cloud passes 1 AU between D1 and S3, and a large SEP event (I1) injects energetic particles into this structure [*Malandraki et al.*, 2002]. Finally, another SEP event (I2) occurs on May 6. The effects of these upstream events (with the possible exception of I2) are observable in the magnetic field and electron measurements from LP.

[13] During this entire time period, the magnitude of negative surface potentials exceeds a typical value of <100 V (see Figure 2c). However, two very large charging events occur almost contemporaneously with the two SEP events (I1, I2). During these two charging events, lunar surface potentials exceed −1 kV, and during the peak of the second event they reach ~−4.5 kV, as in the example shown in Figure 1.

4. Charging Currents

[14] The lunar surface, like any body immersed in plasma, charges so as to minimize the net current to it. For the shadowed lunar surface, the most important currents are those due to ions, electrons, and secondary electrons. During quiet periods, the incident electron current dominates, and the surface charges to a negative potential on the order of the electron temperature [*Manka*, 1973; *Stubbs et al.*, 2007b]. For electron temperatures between a few hundred eV and tens of keV, secondary electron emission may be important [*Horanyi et al.*, 1998], and this represents an important positive current source. During quiet periods, the positive ion current is usually unimportant due to the lower fluxes of ions, but for SEP events this will not generally hold true.

[15] Figure 2b clearly shows that lower energy electrons measured by LP, which usually dominate the charging current balance, cannot explain the extreme charging found during this time period. We observed the highest LP electron fluxes below a few keV at S1, S2, and D3, none of which correspond to the most significant surface charging events (I1, I2). The ER registers significant counts above a few keV at some times that do roughly correspond to the largest surface charging events, but these counts likely consist largely of high energy penetrating particles. By far the largest electron fluxes are found below a few keV, so it may seem surprising that these particles do not control the surface charging. However, electrons in this energy range also produce the most secondaries, potentially mitigating their effect on surface charging by contributing a balancing positive current source.
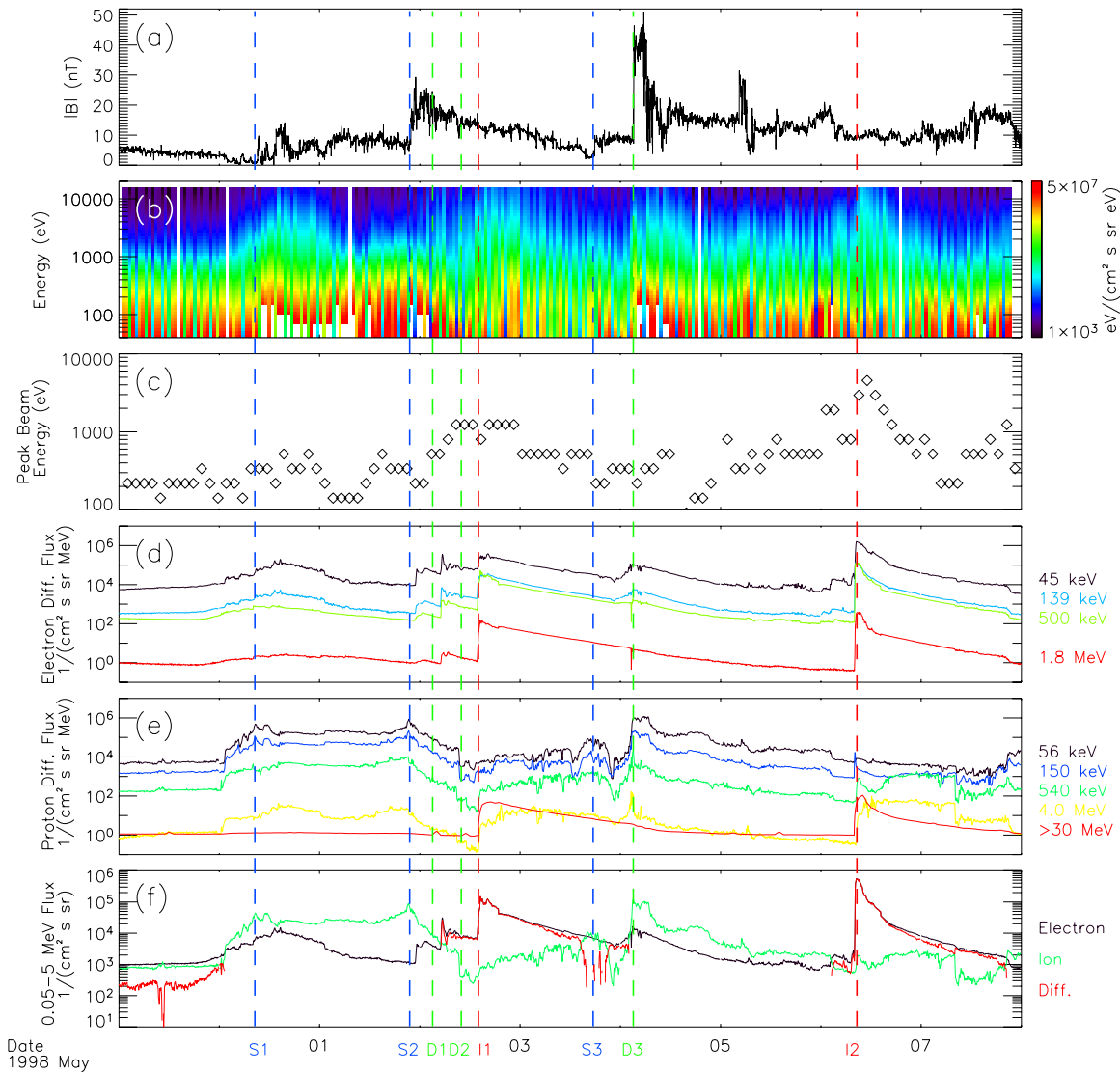
Figure 2. Data from April 29 – May 07, showing magnetic field magnitude, electron differential energy flux and peak beam energy measured by LP, as well as electron and proton differential fluxes measured upstream by SOHO and ACE, and total upstream fluxes integrated over the energy range 0.05–5 MeV. High energy (>30 MeV) proton fluxes in the fifth panel are in units of total flux (1/(cm² s sr)) rather than differential flux. Times of major shocks (S1, S2, S3), directional discontinuities (D1, D2, D3), and SEP injections (I1, I2) indicated by dashed bars.

[16] Figures 2d and 2e suggest that the largest surface charging events during this time period are instead roughly correlated with electron fluxes from 50 keV to a few MeV, as well as >30 MeV proton fluxes. We therefore calculated rank correlations between peak beam energy and upstream charged particle fluxes at all energies. We found significant positive rank correlations with electron fluxes from 40 keV – 5 MeV, and significant negative rank correlations with proton fluxes from 40 keV – 2 MeV (coefficients as high as 0.36, corresponding to less than a 0.01% probability that they arise purely by chance). Surprisingly, proton fluxes above 30 MeV displayed positive rank correlations. This may result from the fact that 30 MeV protons have the same speed as 750 keV electrons, and therefore arrive at the Moon at the same time, possibly with similar time profiles.

[17] The positive correlation with electrons and negative correlation with ions suggest that the Moon is indeed charging in response to the total plasma current to its surface, as expected. We therefore calculated the total flux of electrons minus the total flux of ions over the energy range of 50 keV – 5 MeV, utilizing both ACE and SOHO data. We show the results in the Figure 2f, demonstrating that the largest negative surface charging events roughly correspond to times when the electron flux exceeds the ion flux (implying a net negative current to the surface) as we might expect. Furthermore, we calculate a rank correlation coefficient of 0.54, corresponding to a probability of 1.6×10^{-9} that the correlation arises purely by chance. Clearly, if electrons and ions of these energies completely explained the surface charging, the correlation should be even higher. However, we have neglected charged particles above 5 MeV and below 50 keV, as well as secondary emission.

[18] Furthermore, we have neglected the screening effects of the lunar wake. The high speed of the solar wind relative
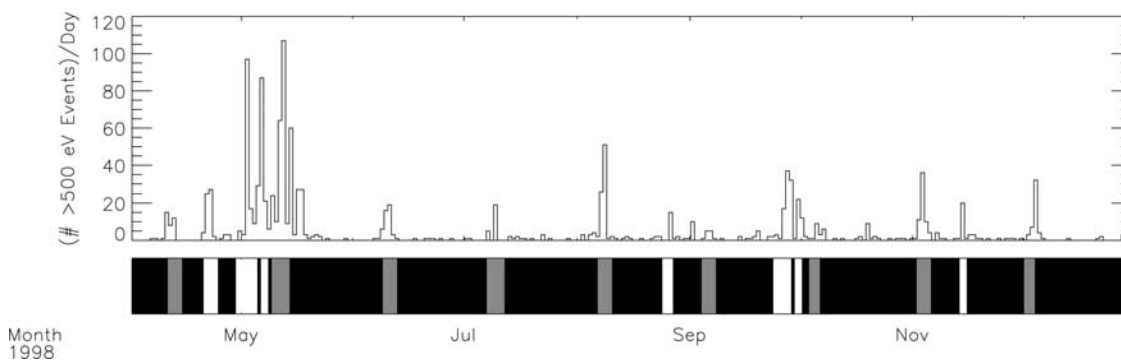
Figure 3. Time series showing number of >500 eV secondary electron beam events per day, with bar indicating times of SEP events (white) and magnetospheric tail passes (grey), for April–December 1998.

to sonic or magnetosonic speeds ensures that thermal ions generally cannot reach the nightside lunar surface. In addition, a significant (∼500 V) ambipolar potential drop exists across the wake boundary in order to maintain quasi-neutrality as solar wind plasma refills the wake, ensuring that thermal electrons cannot penetrate the wake either. For an initially non-Maxwellian electron distribution, the resulting velocity filtration has been shown to increase the electron temperature in the wake [*Halekas et al.*, 2005b]. Suprathermal electrons, meanwhile, due to their higher velocities, can more easily penetrate the wake than suprathermal ions, potentially increasing negative charging currents to the surface. The fact that the largest surface potentials generally occur in the central wake suggests that these various wake-related effects may prove important.

5. Occurrence of Extreme Lunar Charging

[19] We used our automated software to search the entire LP data set for extreme surface charging events. We show a representative subset of the results in Figure 3. Surface charging events >500 V are relatively rare; even the highest occurrence rates only correspond to ∼9% of the observations for a given day (the ER measures a full 3-d electron distribution every 80 s). This is because in the solar wind we generally only observe large negative potentials in the central lunar wake, which LP only encounters for a fraction (<∼25%) of every orbit. Furthermore, we can only infer surface potentials when magnetically connected to the surface. This work shows clearly that the vast majority of these rare large negative surface charging events occur during either SEP events or magnetotail passages (when the Moon encounters the plasmasheet, as previously discussed by *Halekas et al.* [2005a]).

6. Conclusions

[20] The lunar surface potential reaches negative values as large as ∼4.5 kV during a series of space weather events in late April and early May of 1998. We found that the largest surface charging events during this time period corresponded to large SEP injections, and in particular to times when the electron flux between 50 keV and 5 MeV exceeded the proton flux over the same energy range, suggesting that the Moon charges mainly in response to currents from high-energy incident charged particles during these events. We searched the entire LP data set for large

negative lunar surface potentials, and found that they occur primarily during magnetotail crossings and SEP events.

7. Implications

[21] Large surface charging events are hazardous in and of themselves. The record of anomalies and failures on all previous spacecraft missions conclusively shows that electrostatic charging and discharges are the leading environmental cause of anomalies and failures in space [*Bedingfield et al.*, 1996], and there is no reason to expect this to be any different on the lunar surface. Furthermore, electrostatic phenomena have a direct impact on dust on the surface, which in turn can significantly affect exploration and in situ resource utilization [see *Stubbs et al.*, 2007a, and references therein]. Finally, extreme charging occurring in conjunction with SEP events represents a combination of two hazards in parallel, and raises the concern that equipment could fail due to electric and/or dust effects just when it is most critical that it work for astronauts seeking shelter from high energy radiation. Magnetotail passages occur at a predictable time every month, but SEP events are inherently unpredictable, increasing the hazard for exploration.

References

Adams, J. H., Jr., and M. M. Shapiro (1985), Irradiation of the Moon by galactic cosmic rays and other particles, in *Lunar Bases and Space Activities of the 21st Century*, edited by W. W. Mendell, pp. 315–327, Lunar and Planet. Inst., Houston, Tex.

Bedingfield, K. L., R. D. Leach, and M. B. Alexander (1996), Spacecraft system failures and anomalies attributed to the natural space environment, *NASA Ref. Publ. 1390*.

Burlaga, L. F., R. M. Skoug, C. W. Smith, D. F. Webb, T. H. Zurbuchen, and A. Reinard (2001), Fast ejecta during the ascending phase of solar cycle 23: ACE observations, 1998–1999, *J. Geophys. Res.*, *106*, 20,957–20,977.

Farrugia, C. J., et al. (2002), Wind and ACE observations during the great flow of 1–4 May 1998: Relation to solar activity and implications for the magnetosphere, *J. Geophys. Res.*, *107*(A9), 1240, doi:10.1029/2001JA000188.

Gold, R. E., S. M. Krimigis, S. E. Hawkins III, D. K. Haggerty, D. A. Lohr, E. Fiore, T. P. Armstrong, G. Holland, and L. J. Lanzerotti (1998), Electron, Proton, and Alpha Monitor on the Advanced Composition Explorer, *Space Sci. Rev.*, *86*, 541–562.

Halekas, J. S., D. L. Mitchell, R. P. Lin, L. L. Hood, M. H. Acuña, and A. B. Binder (2002), Evidence for negative charging of the lunar surface in shadow, *Geophys. Res. Lett.*, *29*(10), 1435, doi:10.1029/2001GL014428.

Halekas, J. S., R. P. Lin, and D. L. Mitchell (2005a), Large negative lunar surface potentials in sunlight and shadow, *Geophys. Res. Lett.*, *32*, L09102, doi:10.1029/2005GL022627.

Halekas, J. S., S. D. Bale, D. L. Mitchell, and R. P. Lin (2005b), Electrons and magnetic fields in the lunar plasma wake, *J. Geophys. Res.*, *110*, A07222, doi:10.1029/2004JA010991.

Horanyi, M., B. Walch, S. Robertson, and D. Alexander (1998), Electrostatic charging properties of Apollo 17 lunar dust, *J. Geophys. Res.*, *103*, 8575–8580.

Malandraki, O. E., E. T. Sarris, L. J. Lanzerotti, P. Trochoutsos, G. Tsiropoula, and M. Pick (2002), Solar energetic particles inside a coronal mass ejection event observed with the ACE spacecraft, *J. Atmos. Sol. Terr. Phys.*, *64*, 517–525.

Manka, R. H. (1973), Plasma and potential at the lunar surface, in *Photon and Particle Interactions With Surfaces in Space*, edited by R. J. L. Grard, pp. 347–361, Springer, New York.

Muller-Mellin, R., et al. (1995), COSTEP—Comprehensive Suprathermal and Energetic Particle Analyser, *Sol. Phys.*, *162*, 483–504.

Stone, E. C., et al. (1998), The Solar Isotope Spectrometer for the Advanced Composition Explorer, *Space Sci. Rev.*, *86*, 357–408.

Stubbs, T. J., R. R. Vondrak, and W. M. Farrell (2007a), Impact of dust on lunar exploration, in *Proceedings of Dust in Planetary Systems 2005*, *Eur. Space Agency Spec. Publ.*, edited by H. Kruger, and A. Graps, in press.

Stubbs, T. J., J. S. Halekas, W. M. Farrell, and R. R. Vondrak (2007b), Lunar surface charging: A global perspective using Lunar Prospector data, in *Proceedings of Dust in Planetary Systems 2005*, *Eur. Space Agency Spec. Publ.*, edited by H. Kruger, and A. Graps, in press.

————————————

D. A. Brain, G. T. Delory, M. O. Fillingim, J. S. Halekas, C. O. Lee, and R. P. Lin, Space Sciences Laboratory, University of California, Berkeley, CA 94720, USA. (jazzman@ssl.berkeley.edu)

W. M. Farrell, NASA Goddard Space Flight Center, Greenbelt, MD 20771, USA.

M. K. Hudson, Department of Physics and Astronomy, Dartmouth College, Hanover, NH 03755, USA.

R. A. Mewaldt, California Institute of Technology, Pasadena, CA 91125, USA.

T. J. Stubbs, Goddard Earth Sciences and Technology Center, University of Maryland Baltimore County, Baltimore, MD 21250, USA.